Available online at www.sciencedirect.com

SCIENCE DIRECT®

Cement and Concrete Research 35 (2005) 57–66

CEMENT AND CONCRETE RESEARCH

Evidence of anomalous thermal expansion of water in cement paste

John J. Valenza II, George W. Scherer*

Princeton University, Civil and Env. Eng./Princeton Institute for the Science and Technology of Materials, E-319 Eng. Quad., Princeton, NJ 08544, USA

Received 4 February 2004; accepted 27 August 2004

Abstract

A comparative study of permeability measurement by thermopermeametry (TPA) and beam bending was performed on cement paste. To bring the two measurements into agreement, it is necessary to recognize that the pore solution has a thermal expansion coefficient about one and a half times that of bulk liquid and to account for viscoelastic stress relaxation during TPA experiments. The anomalous thermal expansion is not accounted for by the presence of ions in the cement paste pore solution.

Keywords: Characterization; Pore solution; Thermal analysis; Expansion; Permeability

1. Introduction

Flow in porous media obeys Darcy's law which states that the flux of fluid is proportional to the gradient in pressure p [1]:

$$J = -\frac{D}{\eta_L}\nabla p = -k\nabla p \quad (1)$$

where D=permeability (units of area), η_L=viscosity of the pore fluid, and we define the permeability coefficient as $k=D/\eta_L$. The permeability coefficient plays a major role in the formation of hydraulic pressure during freezing [2], stresses during drying [3,4], and thermal stress when exposed to rapid temperature changes [5]. Therefore, an accurate estimate of k is essential for predicting the durability of the material.

The conventional technique for determining the permeability coefficient of cementitious materials consists of applying high pressures (~2 MPa) to a volume of fluid above a porous specimen and measuring the volume of fluid that flows through the specimen over time. A consistent measure of k is not obtained until steady state flow is achieved, which takes days or weeks when k is small [6]. Over this time the sample will age and the permeability will change. Furthermore, the high pressure necessary to force fluid through the specimen can compromise the seal around the sample edge, leading to high estimates of the permeability. To avoid the shortcomings of the conventional technique, we have tested thermopermeametry (TPA) [7] and beam bending [8] to measure k. Neither of these techniques requires high pressures, and both provide results in minutes to hours.

A TPA experiment consists of submerging a saturated porous body and observing the dilation of the body as it is exposed to a temperature cycle. When the temperature is raised, the liquid phase expands much more than the solid phase so it tends to flow out of the body. If the heating rate is fast or the permeability is low, the liquid does not have time to escape, so it is forced to expand in the pores. Thermal expansion of the confined fluid places the fluid in compression and the network in tension, causing the network to stretch like a spring. In addition, a gradient in pore pressure forms between the interior of the solid network and its surface. During a subsequent isotherm, the solid network will force liquid out of its pores until ambient pressure is restored throughout the pore space, and the solid retracts to a dimension dictated by its thermal expansion coefficient. Analyzing the kinetics of the dilation permits extraction of

* Corresponding author. Tel.: +1 6092585680; fax: +1 6092581563.
E-mail address: Scherer@Princeton.Edu (G.W. Scherer).

0008-8846/$ - see front matter © 2004 Elsevier Ltd. All rights reserved.
doi:10.1016/j.cemconres.2004.08.022

the permeability coefficient of the solid network and the thermal expansion coefficient of the solid phase.

The beam bending (BB) technique consists of monitoring the load necessary to sustain a fixed deflection on a simply supported, submerged, and saturated beam of porous material. When a sudden deflection is imposed on the beam, a pressure gradient forms in the pore fluid with tension below and compression above the neutral axis (Fig. 1). In response to this gradient, the pore fluid flows in a manner that restores ambient pressure throughout the pore space. As the gradient is diminished and the pressure is reduced, the load necessary to sustain the deflection decays. Analysis of the kinetics of this load relaxation permits determination of the transport, elastic, and viscoelastic properties of the porous medium. The BB technique was substantiated through measurements on Vycor® glass [9], an elastic material whose transport properties are known, and on cement paste, a viscoelastic material [10,11].

Although the beam bending technique yields more information about the behavior of the saturated porous body, it would be impractical to apply to concrete specimens. This limitation is due to the utilization of simple beam theory to analyze a beam bending experiment, which requires that the length to thickness ratio of the beam be ≥10:1. Therefore, a representative volume of concrete with aggregate ranging in size up to 2 cm would have to be ≥0.1-m thick and ≥1-m long, and would weigh >25 kg. It would not be convenient to prepare or test specimens of this size, so a more practical method is needed for determining the permeability of concrete specimens.

Thermopermeametry does not impose any restrictions on sample size and is therefore readily applicable to concrete specimens such as the cylinders (diameter=75–150 mm) routinely used to measure compressive strength. For samples of this size, temperature gradients are likely, so that situation has also been analyzed [7] and investigated [12]. TPA was previously applied to measure the permeability coefficient of both elastic [13] and viscoelastic gels [14] and was shown to give the same k as was found by beam bending [15]. In light of the difference in the mechanical behavior of compliant gels and rigid cement paste, a similar comparative study was performed between BB and TPA to substantiate the use of TPA with cementitious materials. This comparison reported here brought to light anomalous thermal expansion of the pore solution in the fine pores of cement paste. It will be shown that this is not caused by the normal concentration of ions in the cement paste pore solution. In fact, similar behavior was found in previous studies on the thermal expansion of water and deuterium in a silica xerogel [16], and aqueous solutions in porous glasses [17]. Recent dilatometric experiments in this lab [18] confirmed that the thermal expansion coefficient of pore water in cement paste is about one and half times that of bulk water.

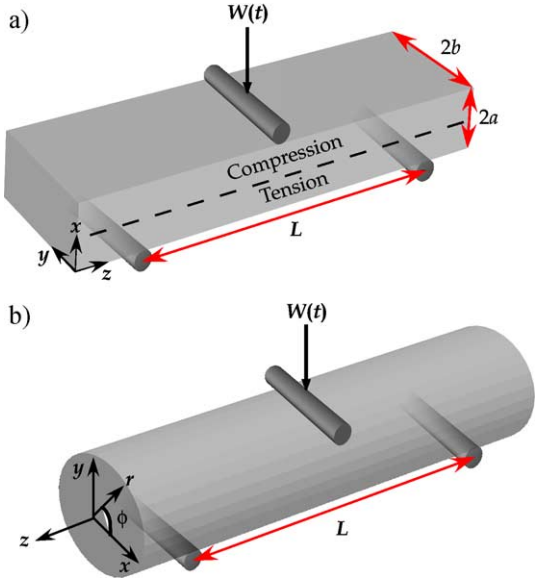

Fig. 1. Schematic of a beam bending experiment on a cement paste specimen of a (a) rectangular cross-section (thickness $2a$) and (b) circular cross-section (radius r).

The next section provides background on the interpretation of the beam bending and TPA experiments. Section 3 discusses details of the beam bending and TPA experimental procedure. Section 4 presents the results of these experiments. A discussion of these results is presented in Section 5.

2. Background

The load necessary to impose and sustain a sudden deflection on an elastic cylindrical beam is [8]:

$$\frac{W(t)}{W(0)} \equiv R = 1 - A + AS\left(\frac{t}{\tau_b}\right). \tag{2}$$

The material parameter A dictates the amount of hydrodynamic relaxation that occurs,

$$A = \frac{\left(\frac{1-2\nu_p}{3}\right)\left(1-\frac{K_p}{K_S}\right)^2}{1-\frac{K_p}{K_S}+(1-\rho)\left(\frac{K_p}{K_L}-\frac{K_p}{K_S}\right)}, \tag{3}$$

$W(0)$ represents the initial load, and the hydrodynamic relaxation function for a cylindrical beam is represented by $S(t/\tau_b)$. The hydrodynamic relaxation time τ_b is

$$\tau_b = \mu_b \frac{\eta_L r^2}{DK_p} \tag{4}$$

where r is the radius of the cylinder. The parameter μ_b is:

$$\mu_b = \left(1-\frac{K_p}{K_S}\right)^2 + \frac{3(1-\rho)}{2(1+\nu_p)}\frac{K_p}{K_L} + \frac{3(\rho - K_p/K_S)}{2(1+\nu_p)}\frac{K_p}{K_S} \tag{5}$$

Minor errors in Ref. [8] in the definitions of the constants A and μ_b are discussed in Refs. [19,20]; the corrected expressions are presented in Eqs. (3) and (5).

The solution for the pressure in the pore fluid as a function of position and time during a BB experiment on an elastic sample of rectangular or square cross-section, $p(x,y,z,t)$, (Fig. 1) is discussed in Ref. [21]. The analysis yields an expression similar to Eq. (2), with $S(t/\tau_b)$ replaced by the product of two relaxation functions, $S_1(t/\tau_b)S_2(\kappa t/\tau_b)$. Furthermore, r is replaced by the sample half thickness a in Eq. (4). To achieve both solutions, it was assumed that no flow occurs along the z-direction (Fig. 1). Therefore, in the cylindrical case, $S(t/\tau_b)$ represents radial flow, and in the rectangular case, $S_1(t/\tau_b)$ represents flow in the x-direction, while $S_2(\kappa t/\tau_b)$ represents flow in the y-direction. The square of the aspect ratio $\kappa=a^2/b^2$ in the argument of S_2 accounts for changes in the relaxation behavior that occur as the rectangular sample gets wider. The validity and accuracy of the analytic expression for predicting the load necessary to sustain a sudden deflection in a BB experiment on a cylindrical [10] or rectangular [11] beam were previously verified.

2.1. Thermopermeametry

The pressure gradient that arises while heating in a TPA experiment is a result of the large difference in the linear thermal expansion coefficient of the pore solution and the solid phase, $\alpha_L \gg \alpha_S$, and the low permeability coefficient k of the cement paste. In TPA experiments, the strain is monitored, so the problem is to predict the strain caused by exposing a sample to a temperature cycle. Consider a large thin plate that lies in the y–z plane (Fig. 2) with its faces at $x=\pm L$, where the strain in the z-direction ϵ_z is monitored. Flow is assumed to occur only perpendicular to the faces, owing to the large aspect ratio of the plate, so the free strain varies only through the thickness of the plate; consequently $\sigma_x=0$, $\sigma_y=\sigma_z$, and $\varepsilon_y=\varepsilon_z$. Inasmuch as there is no external restraint in the z-direction, the force over the edge of the plate must be 0, yielding the following expression for strain in the z-direction, ε_z:

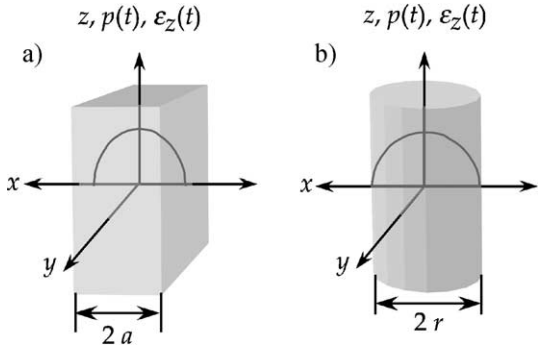

Fig. 2. Schematic of a TPA experiment on a cement paste specimen of a (a) rectangular cross-section (thickness $2a$) and (b) circular cross-section (radius r). Also shown is the pressure gradient, as a function of position x that arises from a change in temperature, ΔT.

$$\varepsilon_z = \varepsilon_s + \alpha_S \Delta T + \left(\frac{\langle p\rangle}{3K_p}\right)\left(1-\frac{K_p}{K_S}\right) \tag{6}$$

where $\langle p\rangle$ is the volume-averaged pressure in the pore fluid

$$\langle p\rangle = \frac{1}{2}\int_{-L}^{L} p(x)\mathrm{d}x. \tag{7}$$

The spontaneous strain ε_s is included to allow for shrinkage from syneresis or other chemical reactions. If present, it would be recognizable as a constant isothermal contraction rate; in our experiments, there was no such shrinkage, so ε_s was ignored in the fits to the data.

The solution for the pressure in a rectangular plate as a function of position and time, $p(x,y,z,t)$, is presented in Ref. [7]. Using this expression for pressure in Eq. (6) yields an implicit solution for ε_z [7]:

$$\begin{aligned}\varepsilon_z - \varepsilon_s + \alpha_S \Delta T = {} & \lambda(1-\beta)b\int_0^\theta \Omega_1^P(\theta-\theta') \\ & \times [\varepsilon_z - \varepsilon_s - \alpha_S \Delta T]\mathrm{d}\theta' \\ & + \lambda\int_0^\theta \Omega_2^P(\theta-\theta')\frac{\partial \varepsilon_T}{\partial \theta'}\mathrm{d}\theta'\end{aligned} \tag{8}$$

where Ω_1^P and Ω_2^P are the relaxation functions. In Eq. (8), $\theta=t/\tau_R$ is the normalized time where the hydrodynamic relaxation time τ_R is:

$$\tau_R = \mu\frac{\beta\eta_L L^2}{DK_p}, \tag{9}$$

The constant μ is given by

$$\mu = \left(1-\frac{K_p}{K_S}\right)^2 + \frac{(1-\rho)}{\beta}\frac{K_p}{K_S} + \frac{(\rho - K_p/K_S)}{\beta}\frac{K_p}{K_S}, \tag{10}$$

and the thermal strain ε_T is the parameter driving the dilation

$$\varepsilon_T = (1-\rho)(\alpha_L - \alpha_S)\Delta T - \varepsilon_s. \tag{11}$$

The two constants β and λ are defined as follows:

$$\beta = \frac{1+\nu_p}{3(1-\nu_p)}, \tag{12}$$

$$\lambda = \frac{\left(1-\frac{K_p}{K_S}\right)}{1-\frac{K_p}{K_S}+(1-\rho)\left(\frac{K_p}{K_L}-\frac{K_p}{K_S}\right)}. \tag{13}$$

For a cylinder whose axis lies along the z-direction, the expression for the expected strain is the same as Eq. (8), with the relaxation functions for a cylinder, Ω_1^C and Ω_2^C, in place of those for a plate and L replaced by the sample radius r in Eq. (9) [7]. The difference in the hydrodynamic relaxation functions is a result of the difference in sample

geometry and represents a difference in flow patterns. Ref. [7] discusses how Eq. (8) is evaluated numerically for fitting the calculated strain to that measured to extract k. Minor errors in the definitions of the constants μ and λ are discussed in Refs. [19,22]; the corrected expressions are presented in Eqs. (10) and (13).

2.2. Viscoelasticity

In BB experiments, cement paste exhibits rapid viscoelastic (VE) stress relaxation. Therefore, in contrast to elastic materials, after hydrodynamic relaxation is complete, the load necessary to sustain the deflection continues to decrease. As a result of this behavior, VE stress relaxation must be accounted for in the solution for $W(t)$. VE stress relaxation in cement paste is accurately represented by [23]:

$$\Psi_{\mathrm{VE}} = \frac{f_2(t)}{1 - f_1(t) + f_2(t)}, \tag{14}$$

where f_1 and f_2 are stretched exponential functions

$$f_k(t) = \exp\left[- \left(\frac{t}{\tau_k} \right)^{b_k} \right], \quad k = 1, 2 \tag{15}$$

and the exponents are b_1=0.18 and b_2=0.35. A rigorous solution of the VE beam bending problem, using the viscoelastic analogy, is presented in Refs. [8,21]. The shape of $W(t)$ is significantly affected by viscoelasticity, even when the average VE relaxation time τ_{VE} is 10^6 times larger than τ_{R}. However, the product of the hydrodynamic and VE relaxation functions (R and Ψ_{VE}, respectively) accurately describes the load relaxation in a beam bending experiment when the relaxation times differ by an order of magnitude ($\tau_{\mathrm{VE}} > 10\tau_{\mathrm{R}}$) [8]. In fact, whenever there is a detectable inflection in $W(t)$ that reveals the end of hydrodynamic relaxation, the approximation $W(t)/W(0) \approx R(t)\Psi_{\mathrm{VE}}(t)$ is valid.

In TPA experiments, the porous network is under stress until the hydraulic gradient is dissipated, so the strain may be affected by creep. A viscoelastic analysis [24] of the TPA experiment indicates that VE stress relaxation is noticeable even if the VE relaxation time τ_{VE} is very large compared to τ_{R} (i.e., $\tau_{\mathrm{R}}/\tau_{\mathrm{VE}} \approx 10^{-5}$). To test for the occurrence of VE stress relaxation during the present TPA experiments, the expected strain was simulated using the VE relaxation parameters and material properties determined during beam bending. The simulated VE response was then analyzed with the elastic solution (Eq. (8)) to determine the error introduced by assuming that the cement paste is behaving elastically.

3. Experimental

3.1. Cement paste specimens

Cylindrical specimens were prepared by Wilasa Vichit-Vadakan for a study reported in Ref. [10]. Type III Portland cement was combined with deionized water at a water-to-cement (w/c) ratio of 0.6 and was cast in standard polystyrene pipettes with an inside diameter of 7.7 mm. Petroleum jelly was used as a mold release agent. After 48 h, the samples were removed from the mold, and excess petroleum jelly was removed from the sample surface with a paper towel. Finally, the samples were placed in a saturated calcium hydroxide solution at room temperature until testing.

Two sets of plates were prepared. Plates of rectangular cross-section were cast with a length of 280 mm and aspect ratios a:b=1:7 and 1:5, as described in Ref. [11]. Another set of plates (S01) was made with only one aspect ratio, a:b=1:7. The plates were cast in polyvinyl chloride (PVC) molds; a removable bottom was aligned and secured along its length with three pins. The gap between the bottom and the mold was sealed with General Electric Silicon I Rubber Sealant to prevent water leakage. The molds were treated with Dupont Krytox® dry film mold release to ensure easy removal of the sample.

All cement paste batches used in making plates were prepared with 740 g of Type III Portland cement and 333 g of deionized water. Material weights were measured with an OHAUS LS5000 balance, with an accuracy of ±2.5 g. The water/cement ratio was w/c=0.45. The cement powder was mixed in a KitchenAid Stand Mixer (Model KSM5PS) on mixer speed 2 (out of 10) for 25 s; then, with the mixer running, the deionized water was added over a period of 10 s. The mixer speed was then increased to 3, and the paste was allowed to mix for 2.5 min. Next, the mixing bowl was removed, and the extremities were scraped with a spatula to ensure uniform mixing. The bowl was remounted, and the paste was mixed on mixer speed 3 for an additional 2 minutes.

After mixing, the paste was placed in a PVC mold and tamped for 1 min to encourage entrapped bubbles to rise. The cement surface was leveled with a screed in a motion perpendicular to the sample length. Finally, excess cement was wiped from the surface of the mold, and a bead of vacuum grease was applied around the edge of the mold. The finished cement surface was then covered with a Plexiglas lid, where the lid was firmly pressed down on the grease to prevent drying. Contact between the vacuum grease or the lid and the cement paste was avoided.

3.2. Porosity

Porosity samples were cut to a length of ~5 cm from companion cylinders and plates. The dimensions of the porosity samples were measured with Mitotuyo calipers with an accuracy of 0.01 mm. The saturated surface dry weights were measured with a Denver Instruments M-220D balance (accuracy=±0.01 mg), and the samples were immediately placed in an oven at 105 °C. The dry weight of the cylindrical samples was taken 48 h later. The dry weight of the plates was monitored periodically.

The porosity found by this method is problematic for two reasons. First, it measures all water that is not chemically bound, so it includes molecules in nanometric pores that might not contribute to the permeability. Inasmuch as the same method was applied to the beam-bending and thermopermeametry samples, comparison of the results of those techniques is valid; however, there might be a significant overestimate of the porosity contributing to the permeability. Secondly, the thermal expansion coefficient of the liquid depends on pore size [17], but we attribute the same value of α_L to all of the liquid in the pores. This is valid because the dilatometric method for measuring α_L also provides the average value for the whole volume of the pore liquid.

3.3. Beam bending

The beam bending apparatus was shown and described in Refs. [9,10]. The displacement of the specimen was measured with a linear variable differential transformer (LVDT, MacroSensors) with a range of 10 mm and a sensitivity of 0.01 μm. The load on the sample was measured with one of two load cells, ±50g or ±250 g (SENSOTEC). Calibration of the load cell and displacement was verified by bending metal beams of known composition. The temperature was monitored with two Type K thermocouples; one taped to the apparatus, one placed in the bath. The apparatus was controlled with a computer running DasyLab 5.0 software (IOTech). The displacement, load, and temperature were logged through a 16-bit A/D converter. Data were recorded at logarithmic intervals of time with an initial sampling rate of 50 Hz.

The sample span L was ~230 mm for cylinders and ~260 mm for rectangular plates. The two sample geometries also required different end supports. Cylinders were supported with V-notch stainless steel supports, consisting of two 6.35-mm diameter rollers set at 90° to one another and 45° to the horizontal plane. Rectangular plates were supported by two cylinders, 6.35 mm in diameter. The pushrod consists of a straight rod that connects to the load cell, runs through the LVDT, and has a cylinder (6.35 mm in diameter) at the end that touches the sample. The pushrod used with the rectangular plates tested in 2002 (F02) had a stainless steel ball (diameter=6.35 mm) at the end that contacts the sample. The supports sat in a stainless steel bath filled with a saturated solution of calcium hydroxide (limewater). Plexiglas plates were placed over the bath in contact with the liquid to suppress waves caused by displacement of the pushrod. The entire apparatus, including the data acquisition hardware, sat in a Forma-Scientific water-jacketed incubator held at 29±0.5 °C.

Prior to performing the experiment, it is necessary to find the sample surface by bringing the pushrod into contact with the sample through small incremental movements. The uncertainty in the position of the probe relative to the sample surface was ±1 μm. The sample was allowed to equilibrate for 1 h to ensure thermal stability and equilibration; the load and position of the pushrod were monitored throughout this time. Five minutes of baseline data were taken at the end of the equilibration period, then a sudden deflection Δ (rectangular plates: Δ=90–150 μm; cylindrical rods: Δ=50–90 μm) was imposed on the sample, and the load necessary to sustain the deflection was measured at logarithmic intervals of time; the displacement stabilized in about 0.7 s. After unloading the specimen and prior to terminating data acquisition, 5 min of baseline data were logged to test for drift in the load cell reading.

3.4. Thermopermeametry

Thermopermeametry experiments were performed with a Perkin-Elmer Dynamic Mechanical Analyzer (DMA) 7e. Samples were cut from rods and plates to a height of 15–17 mm. The sample was placed in the sample holder, and the probe was lowered until it contacted the sample (Fig. 2). The furnace was then raised, submerging the sample in limewater. Water at 0 °C was circulated through a heat exchanger to keep the aluminum block that encompasses the furnace at a constant low temperature (≈6–7 °C). Prior to beginning the analysis, the specimen was allowed to equilibrate at the initial temperature T_0 for 1 h. To ensure thermal stability and equilibration of the sample, the temperature and the probe position were monitored throughout this time. A temperature cycle was then entered with an isotherm at T_0 at the beginning of the experiment to test for the occurrence of autogenous shrinkage. The cylindrical specimens (S01) were exposed to a heating rate of 1 °C/min, while the rectangular specimens (S01 or F02) were exposed to a heating rate in the range 0.2–0.4 °C/min. The dilation of the sample was monitored by the probe, which is connected in line with an LVDT. The temperature of the sample and the aluminum block were monitored with type K thermocouples: one submerged in the limewater close to the sample surface and the other in contact with the block. The error in the measured dilation was verified to be <4% through thermal expansion measurements on aluminum standards.

4. Results

4.1. Porosity

The porosity was determined by the weight loss at 105 °C. The weight loss of the cylindrical specimens was measured after 48 h, and the porosity ϕ was found to be ϕ=0.52. The weight loss of the rectangular specimens was measured periodically; the weight loss stabilized after 24 h, yielding the porosity ϕ=0.45.

4.2. Beam bending

Results of a typical BB experiment are shown in Fig. 3 along with a fit to the data; the extracted hydrodynamic R and viscoelastic Ψ_{VE} relaxation functions are plotted separately. The inflection in the curve corresponds to the end of hydrodynamic relaxation, where R arrives at a plateau. The values of τ_R and A that yield the best fit of Eq. (2) to the measured load relaxation are used to calculate the permeability coefficient from Eq. (4) and the elastic modulus of the specimen [8]:

$$E_p = \frac{W(0)(1-A)L^3}{48\Delta I} \tag{16}$$

respectively. In addition, the values of the two viscoelastic relaxation times, τ_1 and τ_2 (Eqs. (14) and (15)) are adjusted to account for the shape of the load relaxation after hydrodynamic relaxation has ceased.

4.3. Thermopermeametry

The dilation observed during a TPA experiment, along with the fit of the elastic solution for the expected strain (Eq. (8)) and the thermal cycle, is shown in Fig. 4. The elastic modulus extracted from analysis of beam bending on companion samples (Eq. (16)) was used in the analysis of the TPA experiments. A heating rate of 1 °C/min. was used to keep the stress on the body in the linear elastic range, σ_z<1 MPa. The plot clearly shows the overshoot caused by the mismatch in thermal expansion coefficients of the liquid and solid, and the subsequent relaxation during the isotherm resulting from fluid flow alleviating the pressure gradient. During heating, the slope of the curve is decreasing, which indicates that the system is moving toward a steady state. If the system were to reach a steady state, the rate of fluid expansion would be equal to the flux of fluid out of the body. When fitting Eq. (8) to the measured strain, the value of α_S is adjusted to account for the strain at the plateau. The remaining free parameter τ_R is then adjusted to account for the shape of the curve, the height of the peak, and kinetics of

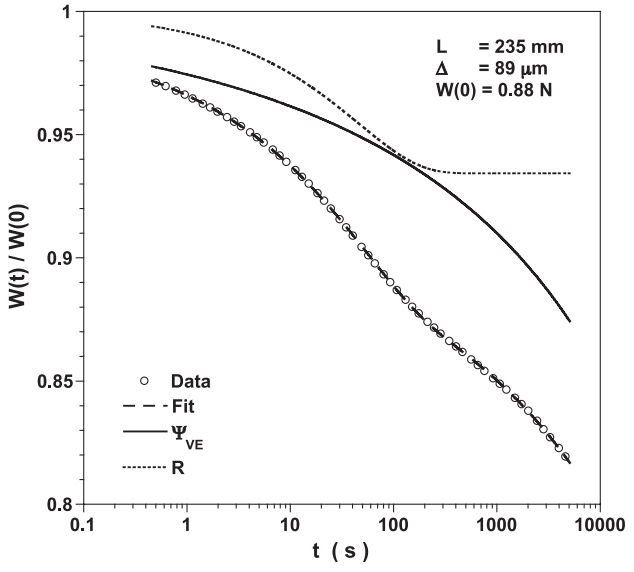

Fig. 3. Result from a typical beam-bending experiment. Plot shows observed load relaxation (symbols) with fit (dashed curve) of Eq. (2) to the data. The hydrodynamic (R) and viscoelastic (Ψ_{VE}) relaxation functions are also shown.

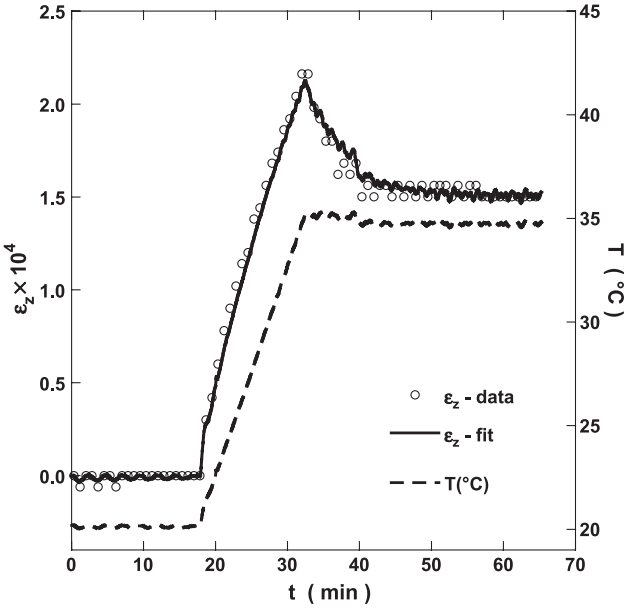

Fig. 4. Result from a typical TPA experiment. Plot shows measured strain (symbols) with fit (solid curve) of Eq. (8) to the data (left ordinate) and the thermal cycle (dashed curve, right ordinate). The heating rate used was 1° C/min. The value of α_L used in the fit was that expected from bulk water in this temperature range α_L=1.0×10^{-4} °C^{-1}.

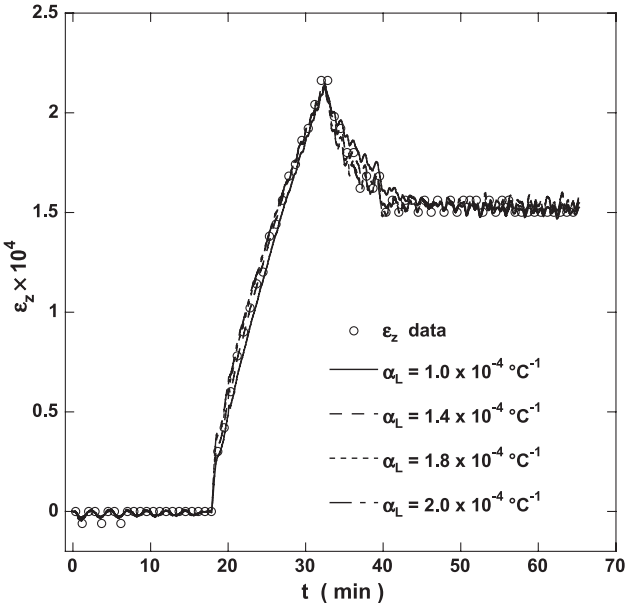

Fig. 5. Fit of the analytical solution for strain (Eq. (8)) to that observed during a TPA experiment on a cylindrical specimen for several values of α_L. The plot illustrates that increasing α_L produces no change in the quality of the fit.

Table 1
Calculated values for the hydrodynamic relaxation time, τ_R, and the corresponding permeability coefficient, k, from analyzing the TPA data shown in Fig. 5 using several values for α_L

α_L ($\times 10^4$ °C^{-1})	τ_R (s)	k (nm^2/Pa·s)
1.0	2048	2.19
1.4	1349	3.33
1.8	983	4.57
2.0	860	5.22

An increase in α_L is offset by a decrease in τ_R, which corresponds to an increase in k.

relaxation to the plateau. The value of τ_R that yields the best fit of Eq. (8) to the measured strain is then used to calculate the permeability coefficient from Eqs. (9) and (10).

4.4. Permeability

The values of k extracted from analysis of TPA data were consistently lower than those determined through beam bending. Inasmuch as the beam bending procedure was substantiated through measurements on porous Vycor® glass [9], the TPA analysis was scrutinized to determine why low estimates of the permeability coefficients were calculated. It was determined that the thermal expansion coefficient of the pore fluid α_L used in the analysis of the TPA data could be increased by a factor of 2 without affecting the quality of the fit (Fig. 5). In addition, we found that increasing the value of α_L used in the analysis yielded smaller values of the fitting parameter τ_R (Table 1), corresponding to larger values of k. Therefore, assuming the pore fluid was expanding anomalously during TPA experiments brought the beam bending and TPA measurements into agreement. Fig. 6 shows this comparison for cylinders, while Fig. 7 illustrates the same for two sets of experiments on rectangular plates. Direct measurements, discussed in Section 5, demonstrated that the expansion of the pore liquid is indeed large.

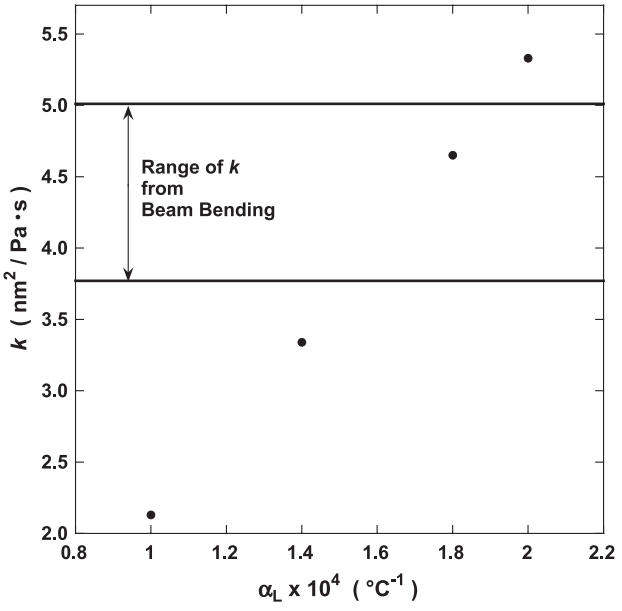

Fig. 6. Comparison of $k=D/\eta_L$ from BB with that extracted from analysis of TPA data (symbols) from cylindrical specimens, using several values for the linear thermal expansion coefficient of the pore liquid α_L. The measurements come into agreement when $\alpha_L \approx 1.6\times10^{-4}$ °C^{-1}.

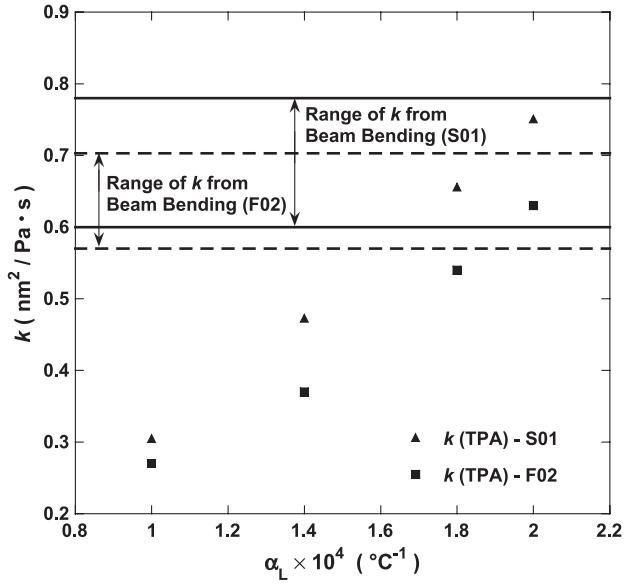

Fig. 7. Comparison of $k=D/\eta_L$ extracted from analysis of TPA data from rectangular plates, using several values for α_L, to that determined through beam bending. The measurements come into agreement when $\alpha_L \approx 1.8\times10^{-4}$ °C.

5. Discussion

Cement paste pore solution contains many dissolved ions including sodium, calcium, potassium, and hydroxyl. Taylor indicates [25] that the concentration of these ions should not climb above 0.7 M. However, data from the literature [26], shown in Fig. 8, indicate that the presence of dissolved ions accounts, at most, for ~20% of the anomalous thermal expansion.

Dissolution of calcium hydroxide crystals or structural changes in the calcium–silicate–hydrate could contribute to the thermal expansion observed in TPA measurements. However, the baseline was found to be flat at constant temperature, so there is no indication of an ongoing reaction. If such effects equilibrated rapidly during heating and cooling, then the resulting strains would simply contribute to α_S. We used a small temperature interval (~15 °C) to minimize chemical or structural changes in our samples during the measurement.

Derjaguin et al. [16] observed anomalously high thermal expansion of water and deuterium in the 5-nm pores of a silica xerogel. The phenomenon is thought to result from the hindered packing of water molecules in nanometric pores. Accordingly, Xu et al. [18] performed a similar measurement in our lab on the thermal expansion of pore solution in cement paste. The value of α_L measured with cement paste

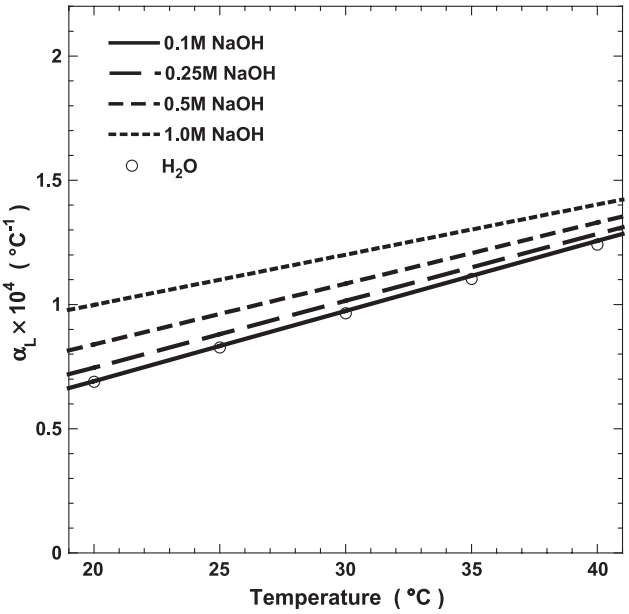

Fig. 8. Plot of the linear thermal expansion coefficient α_L measured for alkali hydroxide solutions of various concentrations; data from Ref. [25] (lines). Also shown is α_L measured on bulk water (symbols); data from Ref. [29].

plates and cylinders is shown in Fig. 9. The thermal expansion of the pore solution in the plates is 60% higher than for bulk water, while thermal expansion of the pore solution in the cylindrical specimens is 30% higher. The difference between the values of α_L measured for plates and cylinders is attributed to the differences in the microstructure of the two geometries, which is demonstrated by

Table 2
Average values for the permeability coefficient, $k=D/\eta_L$, extracted from analyzing beam bending (BB) and thermopermeametry (TPA) experiments on cylinders (CYL) and plates (PLT) with the experimentally determined α_L

Exp. series	Ave. k (BB) (nm^2/Pa · s)	Ave. k (TPA) (nm^2/Pa · s)	Difference (%)
S01 (CYL)	4.65	3.29	29
S01 (PLT)	0.69	0.48	30
F02 (PLT)	0.63	0.41	35

the difference in k (Table 2) determined for the two geometries. The difference in k indicates that the cylinders have a coarser microstructure than the plates, which results in a smaller fraction of the pore fluid exhibiting anomalous expansion. The maximum pore diameter in which anomalous expansion may occur is not yet known for cement paste but is ~15 nm for porous silica glasses [17]. Analyzing the TPA data, using the experimentally determined value of α_L, brings k determined through TPA to within 30–35% (Table 2) of that determined through beam bending.

From the BB results shown in Fig. 3, it is clear that cement paste exhibits rapid VE relaxation. To determine its effect on the TPA experiments, we simulated the VE response to the temperature cycle used in the TPA experiment using k, E_p, and the VE parameters determined through BB, and α_L measured on cement paste. Fig. 10 shows the simulated VE response plotted together with the measured strain. The plot shows that the simulated VE response is identical to the experimental data, which indicates that VE stress relaxation is occurring during the TPA experiment. Note that this is an a priori prediction of the thermal expansion, using independently measured

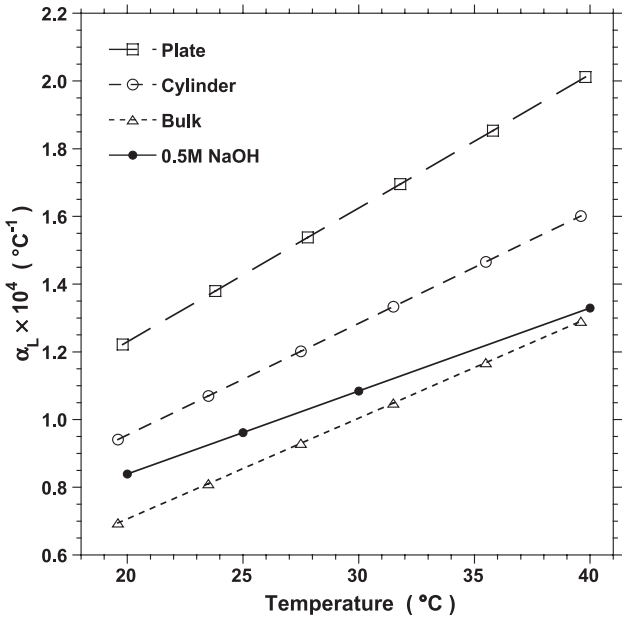

Fig. 9. Measured linear thermal expansion coefficient of the pore fluid in cement paste [18], α_L, compared to that of bulk water [29] in the temperature range of TPA experiments; also shown is α_L measured on 0.5 M NaOH solution [26].

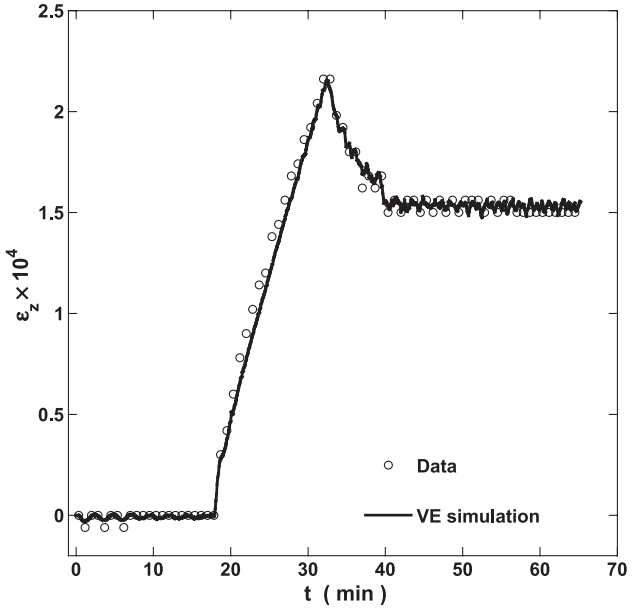

Fig. 10. Plot of measured strain in a TPA experiment on a cylindrical specimen (same as Fig. 4) along with the simulated VE response. The similarity between the data and simulated VE response indicates that VE stress relaxation is occurring during the TPA experiment.

Table 3
Average values for the permeability coefficient $k=D/\eta_L$, used to simulate the VE response (input) and that returned by fitting the elastic solution (Eq. (8)) to the simulated VE response (fit)

Exp. series	Ave. k (input) ($nm^2/Pa \cdot s$)	Ave. k (Fit) ($nm^2/Pa \cdot s$)	Difference (%)
S01 (CYL)	4.65	3.58	23
S01 (PLT)	0.69	0.50	28
F02 (PLT)	0.63	0.45	29

values of α_L, permeability, and mechanical properties, and it yields excellent agreement with the experiment.

To determine the error that would result from assuming elastic behavior, the simulated VE response was fitted to the elastic solution (Eq. (8)), and k yielded by the analysis was compared to that used to simulate the VE response. Table 3 shows that VE stress relaxation accounts for 24–29% of the difference in k determined through BB and TPA. Simulations reported in Ref. [24] show that, for values of the ratio τ_R/τ_{VE} on the order of those found in these experiments, 10^{-4}–10^{-3}, the error introduced by ignoring VE stress relaxation in the analysis of TPA experiments is on the order of 20–30%, which is consistent with our results.

Thus, utilizing the coefficient of thermal expansion measured for the pore fluid and accounting for VE stress relaxation brings k measured through TPA to within 7% of that measured through beam bending. A difference of 7% is well within the experimental uncertainty, considering that the sample-to-sample variation in k measured on cement paste is typically ≈20% [11,27,28]. Ignoring VE relaxation in TPA experiments on cement paste will increase the value of k by a maximum of a factor of 2 (i.e., $k_{fit}/k_{input} \rightarrow 2$ as $\tau_R \rightarrow \tau_{VE}$) [24]. However, VE relaxation in concrete is much less than in cement paste, owing to the reinforcement by rigid aggregate [27], so the neglect of VE relaxation is expected to cause errors much smaller than a factor of 2 for concrete. Furthermore, if the evolution of k is monitored over time, then an error on the order of 30% is insignificant, inasmuch as k may vary by orders of magnitude as the cement paste matures [10,23].

These estimates assume that one also has a means for measuring the coefficient of thermal expansion of the pore solution α_L, a process that diminishes the convenience of the TPA technique. For the range of k discussed in this paper, $5\times10^{-19} < k\ (m^2/Pa\ s) < 5\times10^{-18}$, we have shown that $1.3 < \alpha_L \times 10^4\ (^\circ C^{-1}) < 1.6$, and that α_L is inversely related to k. This is a relatively restricted range of k, but it provides an indication of what value to assume for α_L for all values of k below the upper limit investigated here. For larger values of k, α_L approaches that expected for the normal concentration of ions in the pore solution. Therefore, for k greater than those investigated here, one can comfortably assume that the microstructure is so coarse that no anomalous expansion is occurring. At this time, nothing can be said about the value of α_L expected for values of k below those investigated here; however, systematic measurements are presently underway in our lab to seek a correlation between α_L and k or some other measure of the pore size.

6. Conclusion

The conventional technique for determining the permeability of cementitious materials is time consuming. As a result, we investigated the applicability of the beam bending and thermopermeametry techniques for determining the permeability of these materials. Inasmuch as the BB technique is only applicable to long slender specimens, we performed a comparative study on cement paste to substantiate the TPA technique. The comparison uncovered the occurrence of anomalous thermal expansion of the pore fluid in cement paste, which is thought to result from the hindered packing of water molecules in the small pores of the paste. Accounting for this anomalous expansion and the occurrence of VE stress relaxation during TPA experiments brought the BB and TPA techniques into agreement. Estimates were provided of the extent to which the anomalous expansion and VE stress relaxation affect the TPA results. We conclude that the TPA technique is a convenient viable option for measuring the permeability of cementitious materials.

Acknowledgment

This work was supported by the National Science Foundation Grant CMS-0070092. The authors thank S. Xu and D. Sweeney for permission to use their data (Fig. 9) in advance of publication.

References

[1] J. Happel, H. Brenner, Low Reynolds Number Hydrodynamics, Martinus Nijhoff, Dordrecht, 1986, pp. 389–404.
[2] T.C. Powers, The air requirement of frost resistant concrete, Proc. Highway Res. Board 29 (1949) 184–211.
[3] G.W. Scherer, Theory of drying, J. Am. Ceram. Soc. 73 (1) (1990) 3–14.
[4] G.W. Scherer, Fundamentals of drying and shrinkage, in: V.E. Henkes, G.Y. Onoda, W.M. Carty (Eds.), Science of Whitewares, Am. Ceram. Soc., Westerville, OH, 1996, pp. 199–211.
[5] H. Ai, J.F. Young, G.W. Scherer, Thermal expansion kinetics: method to measure permeability of cementitious materials: II. Application to hardened cement paste, J. Am. Ceram. Soc. 84 (2) (2001) 385–391.
[6] A.S. El-Dieb, R.D. Hooton, A high pressure triaxial cell with improved measurement sensitivity for saturated water permeability of high performance concrete, Cem. Concr. Res. 24 (5) (1994) 854–862.
[7] G.W. Scherer, Thermal expansion kinetics: method to measure the permeability of cementitious materials: I. Theory, J. Am. Ceram. Soc. 83 (11) (2000) 2753–2761.
[8] G.W. Scherer, Measuring permeability of rigid materials by a beam-bending method: I. Theory, J. Am. Ceram. Soc. 83 (9) (2000) 2231–2239.

[9] W. Vichit-Vadakan, G.W. Scherer, Measuring permeability of rigid materials by a beam bending method: II. Porous Vycor, J. Am. Ceram. Soc. 83 (9) (2000) 2240–2245.
[10] W. Vichit-Vadakan, G.W. Scherer, Measuring permeability of rigid materials by a beam-bending method: III. Cement paste, J. Am. Ceram. Soc. 85 (6) (2002) 1537–1544.
[11] J.J. Valenza, G.W. Scherer, Measuring permeability of rigid materials by a beam-bending method: V. Isotropic rectangular plates of cement paste, J. Am. Ceram. Soc. (2004) (in press).
[12] J.P. Ciardullo, D.J. Sweeney, G.W. Scherer, Thermal expansion kinetics: method to measure the permeability of cementitious materials: IV. Effect of thermal gradients, J. Am. Ceram. Soc. (2004) (in press).
[13] G.W. Scherer, Measuring permeability by the thermal expansion method for rigid or highly permeable gels, J. Sol-Gel Sci. Technol. 3 (1994) 31–40.
[14] G.W. Scherer, Thermal expansion of a viscoelastic gel, J. Sol-Gel Sci. Technol. 4 (1995) 169–177.
[15] G.W. Scherer, Bending of gel beams: method of characterizing mechanical properties and permeability, J. Non-Cryst. Solids 142 (1–2) (1992) 18–35.
[16] B.V. Derjaguin, V.V. Karasev, E.N. Khromova, Thermal expansion of water in fine pores, J. Colloid Interface Sci. 109 (2) (1986) 586–587.
[17] S. Xu, G.C. Simmons, G.W. Scherer, Thermal expansion and viscosity of confined liquids, Dynamics of Small Confining Systems, Mat. Res. Soc. Symp. Proc., vol. 790, Materials Res. Soc, Warrendale, 2004, pp. 85–91.
[18] S. Xu, D. Sweeney, G.W. Scherer, Direct measurement of anomalous thermal expansion of water in cement paste, in preparation.
[19] G.W. Scherer, Characterization of saturated porous bodies, Concr. Sci. Eng. 37 (265) (2004) 21–30.
[20] G.W. Scherer, Erratum for 'Measuring permeability of rigid materials by a beam-bending method: I. Theory', G.W. Scherer, J. Am. Ceram. Soc. 83 (9) (2000) 2231–2339, J. Am. Ceram. Soc. 87 (8) (2004) 1612–1613.
[21] G.W. Scherer, Measuring permeability of rigid materials by a beam-bending method: IV. Transversely isotropic material, J. Am. Ceram. Soc. 87 (8) (2004) 1517–1524.
[22] G.W. Scherer, Erratum for 'Thermal expansion kinetics: method to measure permeability of cementitious materials: I. Theory', G.W. Scherer, J. Am. Ceram. Soc. 83 (11) (2000) 2753–2761, J. Am. Ceram. Soc. 87 (8) (2004) 1609–1610.
[23] W. Vichit-Vadakan, G.W. Scherer, Measuring permeability and stress relaxation by beam-bending, Cem. Concr. Res. 33 (2003) 1925–1932.
[24] G.W. Scherer, Thermal expansion kinetics: method to measure permeability of cementitious materials: III. Effect of viscoelasticity, J. Am. Ceram. Soc. 87 (8) (2004) 1509–1516.
[25] H.F.W. Taylor, Cement Chemistry, Thomas Telford, London, 1997, p. 213.
[26] J.M. Simonson, R.J. Ryther, Volumetric properties of aqueous sodium hydroxide from 273.15 to 348.15 K, J. Chem. Eng. Data 34 (1989) 57–63.
[27] A.M. Neville, Properties of Concrete, 4th ed., Wiley, London, 1996, p. 494.
[28] R.D. Hooton, A.S. El-Dieb, Evaluation of water permeability of high performance concrete, Proceedings of the International Conference on Concrete Under Severe Conditions, Sapporo, Japan, 1995, pp. 422–432.
[29] A. Apelblat, E. Manzurola, Volumetric properties of water, and solutions of sodium chloride and potassium chloride at temperatures from T=277.15 K to T=343.15 K at molalities of (0.1, 0.5, and 1.0) $mol \cdot kg^{-1}$, J. Chem. Thermodyn. 31 (1999) 869–893.